

The Linear Q and the Calculation of Decaying Spherical Shocks in Solids*

J. A. VIECELLI

Lawrence Livermore Laboratory, University of California, Livermore, California 94550

Received March 7, 1972

The effect of the linear Q on the decay of a spherical shock wave in a solid, as calculated by Lagrangian finite difference techniques, is determined by a study of the partial differential equations approximated by the difference equations. It is shown that the computed solutions approach an asymptotic form determined by the linear Q terms, and the decay law imposed by the linear Q is given. Finally, it is suggested that the physics of the weak decaying shock problem indicate that the numerical linear Q needs to be replaced by terms modeling a true physical damping mechanism.

INTRODUCTION

A computational physics problem in explosion technology is the accurate calculation of a decaying spherical shock wave in a solid. A particular example currently under investigation is the accurate calculation of surface spallation resulting from the detonation of a contained nuclear explosion. The velocity of the spall is twice the particle velocity of the incident shock wave, hence the determination of spall velocity depends on accurate calculation of particle velocity. In addition to military applications, accurate calculation of decaying shocks in solids is necessary for such technologies as the nuclear explosion stimulation of gas and oil wells.

A characteristic of an explosion contained by a solid, almost always the earth, is that the pressure and particle velocity decays rapidly with increased distance from the detonation point. Thus, not far from the explosion, the material response of the medium is nearly linear in the sense that the convective terms in the Eulerian description of momentum conservation are small compared with the pressure terms. Blast waves that satisfy this condition are called weak decaying shocks in the remainder of the paper.

Computer programs, based on finite difference approximations to the differential equations of motion, have been used to calculate shock waves in solids [1-4]. These

* This work was performed under the auspices of the U. S. Atomic Energy Commission.

programs integrate the following Lagrangian equations of motion in two spatial dimensions with axial symmetry:

$$\frac{\partial u}{\partial t} = -\frac{1}{\rho} \frac{\partial P}{\partial R} + \frac{1}{\rho} \frac{\partial \tau_{RZ}}{\partial Z} + \frac{1}{\rho} \frac{\partial \tau_R}{\partial R} + \frac{2\tau_R + \tau_Z}{\rho R} + G_R \quad (1)$$

$$\frac{\partial v}{\partial t} = -\frac{1}{\rho} \frac{\partial P}{\partial Z} + \frac{1}{\rho} \frac{\partial \tau_{RZ}}{\partial R} + \frac{1}{\rho} \frac{\partial \tau_Z}{\partial Z} + \frac{\tau_{RZ}}{\rho R} + G_Z \quad (2)$$

$$\frac{\partial \tau_R}{\partial t} = \frac{2\mu}{3} \left(2 \frac{\partial u}{\partial R} - \frac{\partial v}{\partial Z} - \frac{u}{R} \right) \quad (3)$$

$$\frac{\partial \tau_Z}{\partial t} = \frac{2\mu}{3} \left(2 \frac{\partial v}{\partial Z} - \frac{\partial u}{\partial R} - \frac{u}{R} \right) \quad (4)$$

$$\frac{\partial \tau_{RZ}}{\partial t} = \mu \left(\frac{\partial u}{\partial Z} + \frac{\partial v}{\partial R} \right) \quad (5)$$

$$\frac{\partial R}{\partial t} = u \quad (6)$$

$$\frac{\partial Z}{\partial t} = v. \quad (7)$$

Here R is the radial coordinate, Z is the axial coordinate, u is the radial component of velocity, v is the axial component of velocity, t is the time, ρ is the density, P is the pressure, G_R and G_Z are the components of gravitational acceleration, τ_R , τ_Z and τ_{RZ} are the deviatoric stresses, and μ is the shear modulus. The equation of state is usually in the form:

$$P = f(\Theta), \quad \Theta = \frac{\rho}{\rho_0} - 1. \quad (8)$$

The density of a zone in the finite-difference approximation is determined by dividing the mass of the Lagrangian zone (which remains constant throughout the calculations) by the volume of the zone, which in turn, is calculated from the coordinates of the mesh points defining the zone at the current time. Yield and failure are incorporated by altering the stresses τ_R , τ_Z , τ_{RZ} at each time step of the integration according to a prescription based on the current state of stress. In the case of elastic behavior, the stresses are left unaltered and the pressure is computed from

$$P = k\Theta, \quad (9)$$

where k is the bulk modulus.

The computer programs for solving these equations, such as the TENSOR program [1, 2] and the HEMP program [3, 4], rely on different finite-difference

approximations to the above partial differential equations. However, they have one feature common to all elastic-plastic Lagrangian difference codes: the substitution of $P + Q$ for P where Q is the "pseudo-viscosity" introduced by Von Neumann (see Richtmyer [5]). The purpose of Q is to provide a mechanism by which kinetic energy can be converted to internal energy as the material is shocked. In the case of motion in one spatial dimension, the quadratic Q is intended for very strong shock waves and has the form

$$Q = \begin{cases} C_0 \rho (\Delta x)^2 \left(\frac{\partial u}{\partial x} \right)^2 \frac{\partial u}{\partial x} < 0 \\ 0 & \frac{\partial u}{\partial x} > 0, \end{cases} \quad (10)$$

where ρ is the density, C_0 is a constant of the order of one, and Δx is the size of the spatial difference interval.

As noted earlier, the spherical shock wave from an explosion in a solid decays rapidly with distance. As a result, one quickly reaches a range at which quadratic, or second order, terms become small compared with the first order terms in the difference equations of motion. To counteract this, investigators have added linear or first order terms to the expression for Q . There have been many formulations of Q but a fairly typical example in one spatial dimension is

$$Q = \begin{cases} C_0 \rho (\Delta x)^2 \left(\frac{\partial u}{\partial x} \right)^2 - C_1 \rho \alpha \Delta x \left(\frac{\partial u}{\partial x} \right) \frac{\partial u}{\partial x} < 0 \\ -C_1 \rho \alpha \Delta x \left(\frac{\partial u}{\partial x} \right) & \frac{\partial u}{\partial x} > 0, \end{cases} \quad (11)$$

where C_1 is a constant, α is the compressional sound velocity, and Δx is the mesh width. As the wave decays, the linear terms in this Q remain comparable to the other terms in the equations of motion and continue to perform the function of converting the kinetic energy of oscillation between neighboring mesh points into internal energy.

In fact, the inclusion of linear Q terms amounts to adding dissipation terms to the basic differential equations. If one defines the viscosity coefficient $\eta \equiv C_1 \rho \alpha \Delta x$ and takes the limit $\Delta t \rightarrow 0$, $\Delta R \rightarrow 0$, $\Delta Z \rightarrow 0$ while holding η constant, the difference equations approach the differential equations for the Voigt-Kelvin model of a viscoelastic solid. In practice, one almost always operates with a value of C_1 such that η is large enough that the Q terms dominate any of the truncation effects arising from the difference approximation to the other terms in the differential equations. For this reason, the solutions obtained from the difference equations approach very closely the solutions one obtains for the differential equations with dissipation terms added.

The intent of this paper is to provide a quantitative understanding of the effect of the linear Q upon the attenuation of a weak spherical shock. Because the phenomena is so nearly linear, except in the immediate neighborhood of the explosion, it is easier to attack the problem at the level of the partial differential equations rather than that of the difference equations. The specific Q investigated is used in a version of the TENSOR program [1, 2]. The critical role Q plays in determining the pulse shape and particle velocity in a weak spherical shock will be demonstrated, and it will be shown that the presence of a linear Q implies an inverse three-halves power decay law.

ASYMPTOTIC SOLUTION FOR THE SPHERICAL SHOCK WITH LINEAR Q

With the tensor version of the linear Q used in the program, the differential equations are

$$\frac{\partial u}{\partial t} = -\frac{1}{\rho} \frac{\partial(P + Q - \tau_R - Q_R)}{\partial R} + \frac{1}{\rho} \frac{\partial(\tau_{RZ} + Q_{RZ})}{\partial Z} + \frac{2\tau_R + \tau_Z + 2Q_R + Q_Z}{\rho R} \quad (12)$$

and

$$\frac{\partial v}{\partial t} = -\frac{1}{\rho} \frac{\partial(P + Q - \tau_Z - Q_Z)}{\partial Z} + \frac{1}{\rho} \frac{\partial(\tau_{RZ} + Q_{RZ})}{\partial R} + \frac{\tau_{RZ} + Q_{RZ}}{\rho R}, \quad (13)$$

where τ_R , τ_Z , and τ_{RZ} are the deviatoric stresses and the Q , Q_R , Q_Z , and Q_{RZ} are given by

$$Q_R = \frac{2\eta}{3} \left(2 \frac{\partial u}{\partial R} - \frac{\partial v}{\partial Z} - \frac{u}{R} \right), \quad (14)$$

$$Q_Z = \frac{2\eta}{3} \left(2 \frac{\partial v}{\partial Z} - \frac{\partial u}{\partial R} - \frac{u}{R} \right), \quad (15)$$

$$Q_{RZ} = \eta \left(\frac{\partial u}{\partial Z} + \frac{\partial v}{\partial R} \right), \quad (16)$$

$$Q = -\lambda \left(\frac{\partial v}{\partial Z} + \frac{1}{R} \frac{\partial u R}{\partial R} \right); \quad (17)$$

$$\eta = C_1 \rho^\alpha \langle \Delta x \rangle, \quad (18)$$

$$\lambda = C_1 \rho^\alpha \langle \Delta x \rangle. \quad (19)$$

Here $\langle \Delta x \rangle$ is the characteristic mesh length and C_1 is an input constant. In a two-dimensional calculation $\langle \Delta x \rangle$ is determined from a weighted average of the

distances between the mesh points defining a zone. In one-dimensional calculations $\langle \Delta x \rangle$ is just the width of a zone. Although η and λ are numerical and not physical quantities, the notation denoting shear viscosity and bulk viscosity has been used to emphasize the equivalence of the linear Q formulation to the Voigt-Kelvin model of a viscoelastic solid.

The deviatoric stresses are determined by the original Eqs. (3-5). With the assumption of small displacements, the spatial differentials with respect to the Lagrangian coordinates may be replaced by spatial differentials with respect to Eulerian coordinates. Substitution of Eqs. (6 and 7) into Eqs. (3-5, 14-16, and 17) and, in turn, substitution of these equations and Eq. (9) into Eqs. (12 and 13) results in a pair of linear partial differential equations for the Lagrangian displacements ΔR and ΔZ . In the theory of elasticity it is shown that the elastic displacement equations can be further simplified by the introduction of scalar and vector potentials. In the case of spherical symmetry the vector potential is zero and one need only solve for the scalar displacement potential given by

$$\frac{\partial^2 \phi}{\partial t^2} = \left(\frac{k + \frac{4\mu}{3}}{\rho} \right) \frac{1}{r^2} \frac{\partial}{\partial r} \left(r^2 \frac{\partial \phi}{\partial r} \right) + \left(\frac{\lambda + \frac{4\eta}{3}}{\rho} \right) \frac{1}{r^2} \frac{\partial}{\partial r} \left(r^2 \frac{\partial^2 \phi}{\partial r \partial t} \right). \quad (20)$$

The radial displacement is then given by

$$\Delta R = - \frac{\partial \phi}{\partial r}. \quad (21)$$

The velocity potential is given by

$$\Phi = \frac{\partial \phi}{\partial t}, \quad (22)$$

so that the particle velocity is given by

$$u = - \frac{\partial^2 \phi}{\partial r \partial t}. \quad (23)$$

In deriving the basic differential equation corresponding to the spherical shock problem with the linear Q , I have taken the coefficients η and λ to be constants while, in fact, they usually have some spatial variation as a result of variations in the mesh width, density, and sound speed. Furthermore, I have used a linear Q that is effective in both compression and expansion regions; in many formulations the linear Q is set to zero in expansion regions. The version of the TENSOR program used has constant input values for η and λ and leaves the linear Q on in expansion regions so that all of the requirements for the analytic solution are strictly satisfied.

The driving mechanism that approximates the explosion closely at early times is that of a small cavity expanding at constant velocity. This boundary condition is satisfied if the solution approaches the form

$$\phi = \frac{\phi_0 t}{r} \quad (24)$$

in the neighborhood of the origin. To solve for the asymptotic form of the decaying spherical shock with linear Q , put $\phi = A/r$ and substitute into Eq. (18) to get

$$\frac{\partial^2 A}{\partial t^2} = \alpha^2 \frac{\partial^2 A}{\partial r^2} + \nu \frac{\partial^3 A}{\partial r^2 \partial t}, \quad (25)$$

where

$$\alpha^2 = \frac{k + \frac{4}{3}\mu}{\rho} \quad (26)$$

and

$$\nu = \frac{\lambda + \frac{4}{3}\eta}{\rho}. \quad (27)$$

Taking the Laplace transform H of A with respect to time gives

$$s^2 H - sA(0) - A(0) = \alpha^2 \frac{\partial^2 H}{\partial r^2} + \nu \frac{\partial^2}{\partial r^2} \{sH - A(0)\}. \quad (28)$$

Since the material is initially at rest, A and \dot{A} are identically zero, thus

$$\frac{d^2 H}{dr^2} - \left(\frac{s^2}{\alpha^2 + \nu s} \right) H = 0. \quad (29)$$

The solution, which decays to zero as $r \rightarrow \infty$, is

$$H(r, s) = A(s) \exp\{-rs(\alpha^2 + \nu s)^{-1/2}\}. \quad (30)$$

The Laplace transform of the boundary condition at $r = 0$ is

$$L\{\phi_0 t\} = \phi_0 s^{-2}. \quad (31)$$

Therefore, the transform of the solution is

$$H(r, s) = \phi_0 s^{-2} \exp\{-rs(\alpha^2 + \nu s)^{-1/2}\}. \quad (32)$$

Taking the time derivative of the solution corresponds to multiplying the transform of the solution by s , since $A(+0) = 0$, therefore the transform of \dot{A} is

$$F(r, s) = \phi_0 s^{-1} \exp\{-rs(\alpha^2 + \nu s)^{-1/2}\}. \quad (33)$$

The inversion may be performed easily when

$$\frac{r\alpha}{2\nu} \gg 1,$$

corresponding to the asymptotic limit to give the velocity potential

$$\Phi(r, t) = A/r = \frac{\phi_0}{2r} [1 + \operatorname{erf}(\tau \sqrt{\sigma})], \quad (34)$$

where

$$\tau = \frac{\alpha t}{r} - 1 \quad (35)$$

and

$$\sigma = \frac{r\alpha}{2\nu}. \quad (36)$$

Therefore the solution for the particle velocity is

$$u = \frac{\phi_0}{2r^2} \left\{ 1 + \operatorname{erf}(\tau \sqrt{\sigma}) + (2 + \tau) \left(\frac{\sigma}{\pi} \right)^{1/2} \exp(-\sigma\tau^2) \right\}. \quad (37)$$

DISCUSSION OF RESULTS

The analytic solution has been evaluated for a particular case and the results are plotted as small circles in Fig. 1. The parameters for this case are $\phi_0 = 1.6 \times 10^8 \text{ cm}^3 \text{ sec}^{-1}$, $\nu = 7.5 \times 10^7 \text{ cm}^2 \text{ sec}^{-1}$, $\alpha = 2.3 \text{ km sec}^{-1}$, and $t = 0.35 \text{ sec}$. Figure 1 also includes the results for a TENSOR calculation of the same problem. These are plotted as small crosses. The elastic constants enter into the analytic solution only by way of the compressional sound velocity, thus there are two additional variables in the finite-difference problem. These are the density and Poisson's ratio, which I chose to be 2.0 g cm^{-3} and $1/3$, respectively. The choice is arbitrary, since once these two variables are fixed, the bulk modulus and shear modulus are determined by the sound velocity.

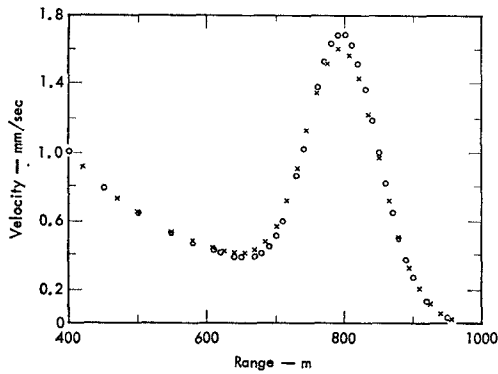


FIG. 1. Shock particle velocity plotted as a function of range. The small circles are points evaluated from the analytic solution. The crosses are points obtained from a finite-difference solution. The time is 0.35 sec.

Spherical symmetry was simulated in the numerical problem by choosing a wedge-shaped mesh with one edge along the z axis of axial symmetry and the other edge at an angle of 10 deg from the z axis. The wedge began at an inner radius of 20 m and extended out to 1150 m. The analytic result is the asymptotic solution for a cavity expanding at constant velocity. Thus it is necessary to start the numerical calculation with a cavity small enough to ensure that the asymptotic state is reached before comparing results. Furthermore, the cavity must not be driven with too large a velocity, else the linearity assumption would be violated. These precautions must be taken to guarantee that the source function in the numerical problem is well defined in terms of the source in the analytical solution.

It should be emphasized that the asymptotic state is eventually reached whether or not the linearity assumption is violated in the neighborhood of the cavity. For a nonlinear source, there is always some particular amplitude for the linear source that produces the same asymptotic state as the original nonlinear source. The precautions mentioned ensure that the numerical problem starts with the equivalent linear source amplitude known beforehand. The cavity velocity corresponding to the value of ϕ_0 in the analytical solution is 40.0 cm sec⁻¹. That value satisfies the analytical boundary condition given by Eq. (24) for an initial cavity radius of 20.0 m.

The numerical calculation was done on a mesh containing 140 radial zones. The zoning was not uniform so as to permit relatively fine zoning next to the cavity. This is necessary to get a good approximation to the analytical source at zero radius. The slight amplitude discrepancy observed in Fig. 1 is the result of this approximation. This was confirmed by making several runs, each with a smaller driving cavity and finer zoning. The amplitude of the numerical solution was

observed to converge to the analytical result as the resolution in the cavity region increased. The zone size at the cavity for the run in Fig. 1 was 2.0 m. The zone size increased gradually to 15.0 m at a radius of 550.0 m. Beyond this radius the zone size remained constant at 15.0 m.

By referring to Eqs. (18), (19), and (27) one can see that beyond 550 m the zone size and the parameters ν and α are equivalent to a linear Q coefficient of 0.1, which is the value normally used in TENSOR calculations. The fact that the computer solution continues to agree with the analytical solution beyond 550 m supports the contention that the linear Q , as actually used in practical calculations, dominates truncation effects arising from other terms in the equations. To check this, the free surface was moved out to 2000 m (with the same 15.0 m zone size) and the calculation continued until the pulse reached 1500 m. At the greater range, the pulse approaches a symmetrical Gaussian form, similar to the example shown in Fig. 2, but the close agreement between computer and analytical solutions is maintained.

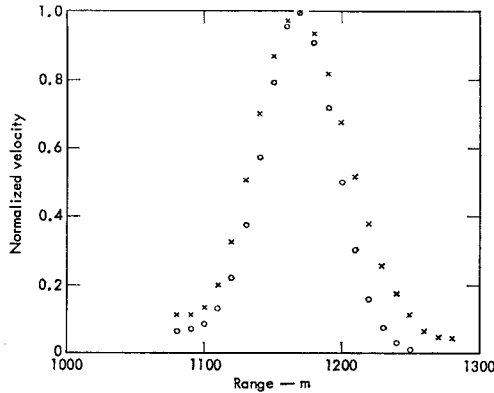


FIG. 2. Normalized shock particle velocity plotted as a function of range. The small circles are points evaluated from the analytic solution. The crosses are points obtained from the finite-difference solution. The time is 0.375 sec.

An indication of how closely an actual explosion calculation approaches the asymptotic form imposed by the linear Q is given by the particle velocity plot in Fig. 2. The TENSOR finite-difference results are indicated by the small crosses and the asymptotic solution by the small circles. The numerical calculation simulated the explosion of a 25.0 kton explosion in the earth at a depth of 1280 m. The source was a spherical cavity, initially with a radius of 5.0 m, containing vaporized rock at a pressure of 1.74 mbar. The gas expanded adiabatically, forcing the walls of the cavity out to a radius of approximately 30 m. The containing rock was

programmed to have a shear strength of only a few kilobars, hence severe plastic flow occurred. In addition, the numerical simulation included overburden and several different layers of earth and rock materials, so that the portion of the shock propagating vertically passed through a density and strain energy gradient. It is not necessary to go further into the details of the numerical run except to note that the average values of α and ν were $3.12 \times 10^5 \text{ cm sec}^{-1}$ and $1.85 \times 10^7 \text{ cm}^2 \text{ sec}^{-1}$, respectively. These values were used in evaluating the analytical solution. The plot shown in Fig. 2 was taken along a radius, which extended vertically to the surface, located at 1280 m. The failure of the numerical solution to go to zero on the leading side of the pulse is explained by the fact that the shock is just beginning to strike the surface. Despite all of the nonlinearities, and inelastic behavior in the source region the resulting blast wave is in close agreement with the predictions of the asymptotic linear theory.

The development and discussion has been based on a formulation of the linear Q which is active in both compression and expansion zones, however many investigators simply turn the linear Q off in expansion regions maintaining that there should not be a dissipative mechanism there. An analytical solution for this type of linear Q might be derivable by perturbation methods, but I was not able to do it. To examine this case, the first problem (the run shown in Fig. 1) was rerun with the Q terms set to zero in expansion regions. Figure 3 is a duplicate of Fig. 1 with the addition of the run with the Q turned off in expansion. It can be seen that this run is the same as the first except in the expansion region where the removal of the linear Q has introduced an oscillatory perturbation. The decay rate for the run with the Q turned off in expansion was observed to follow an inverse 1.5 power law.

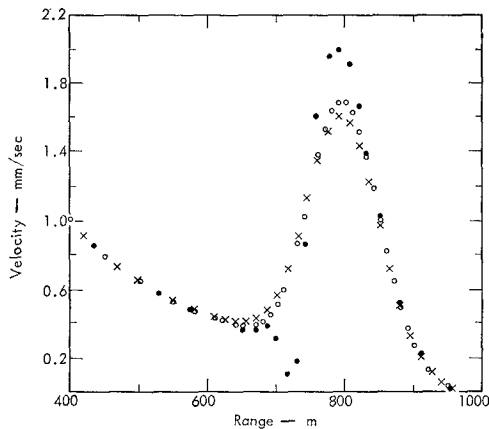


FIG. 3. Duplicate of Fig. 1 with the addition of a run with the linear Q set to zero in expansion regions. Data points from this run are indicated by the solid dots. The time is 0.35 sec.

The intent of this work has been to gain a theoretical understanding of the linear Q and its effect on a weak blast pulse in a solid. The originators of the quadratic Q intended it to be a convenient computational device for including strong shock discontinuities in invicid gas dynamic calculations. Since the physical model assumed invicid flow it was natural to suppress viscosity effects everywhere except at a shock. One of the main reasons for the subsequent development of the linear Q is the fact that unless some kind of linear damping is included in the calculation of weak decaying waves the solutions quickly become obscured in a hashwork of short wavelength noise. The idea that viscosity must be suppressed except at the shock front has persisted through the development of the linear Q , first in applications to gases and then finally to solids.

The underlying physics of weak decaying shocks in solids, and gases also, is different from that of high-pressure, high-speed gas dynamics. In the latter case viscous effects can usually be ignored except in shocks or thin boundary layers. In the former case, at some point in the decay of the shock pulse, the physical attenuation mechanisms come to have a dominant effect on the pulse form and decay rate. A comprehensive discussion of the shock decay process is given by Lighthill [6]. The shock transition region thickens until there is no recognizable shock, just a smoothly varying attenuated sound pulse. In solids and earth materials this point may be very near the site of the explosion. For example, the shock fronts from large nuclear explosions in Nevada Tuffs (a kind of compacted partially fused volcanic ash) are spread over as much as several hundred meters by the time the front has traveled a kilometer. It is at this finite-amplitude sound wave stage that numerical noise becomes a problem unless suppressed by some kind of linear damping mechanism.

In practice the solid mechanics programs cannot compute purely elastic response because the calculations must always be made with a finite number of zones. In the case of decaying explosion waves what they do calculate is the response for a type of Voigt solid, but with viscosity coefficients that depend on purely numerical parameters. The fact that some type of viscosity is required for an adequate physical model of decaying shocks suggests that the use of the linear Q could be made more rational. This could be done by making it correspond exactly to some physical model of damping, rather than have it depend on zone size and shape, and whether or not the zone is in expansion or compression. The easiest thing to do is to make the linear Q correspond exactly to the Voigt model by keeping the Q on in both compression and expansion and by making the coefficients η and λ in Eqs. (14–17) input viscosities.

It is evident from the preceding results that the amplitude and shape of the blast pulse are strongly influenced by a linear Q , so that the spall velocity is also strongly affected. It is, therefore, useless to attempt to calculate spall velocities in weak decaying shock problems without first replacing the linear Q by some physical

model of damping such as the Voigt model. While the Voigt model may not be the best physical model, it is at least free from arbitrary numerical parameters such as zone size and shape. Furthermore, with the Voigt model one can show that a fundamental quantity, the integrated momentum per unit surface area of the pulse, is independent of the viscosity coefficients. Integrating Eq. (37) in the limit of large radius

$$M \sim \frac{\phi_0}{r} \int_{-\infty}^{\infty} \sqrt{\frac{\sigma}{\pi}} e^{-\sigma r^2} d\tau = \frac{\rho \phi_0}{r}. \quad (38)$$

This is an important quantity because it can be measured experimentally and because it is the impulse that can be delivered by the blast pulse if it is absorbed inelastically. In the case of an underground explosion, the surface spall acts as the absorber, carrying most of the momentum of the blast pulse with it as it flies up from the surface. The significance of the result in Eq. (38) is that one can expect to calculate the impulse delivered by the blast wave correctly independent of the viscosity coefficients. Although it may not be possible to calculate the spall velocity correctly because realistic viscosity coefficients are not known or because they must be made abnormally large for numerical smoothing, it should still be possible to correctly calculate the impulse delivered by the blast wave.

Knowledge of the decay law imposed by the damping mechanism is also useful. The decay law for the Voigt model obtained from Eq. (37) is

$$u \sim C_1^{-1/2} r^{-3/2}. \quad (39)$$

This result can be used to infer the decay rate for other types of physical damping mechanisms that may be added to the model. For example, the adiabat and Hugoniot are usually represented by the single curve, Eq. (8), in calculations because physically they are practically identical for many solids not shocked above the melting point. However, some earth materials exhibit porosity, so that after shocking, the material follows a different adiabat lying below the adiabat for the unshocked material. As a result the shock pulse undergoes as additional attenuation in traversing the material, and the decay law follows a higher inverse power than 1.5. The difference can then be ascribed to the porosity.

The results presented in this paper may appear paradoxical. It has been shown that the traditional linear Q is essentially a Voigt viscosity but with nonphysical viscosity coefficients proportional to the spatial difference interval. It has also been demonstrated that the presence of these terms ensures that the late time pulse amplitude follows a viscous decay law. If this is so, then how can the numerical solutions obtained from the traditional linear Q finite difference programs ever converge to the asymptotic solutions for purely elastic response? Obviously, by making the difference interval smaller one reduces the artificial viscosity coefficients

proportionately, but this will not affect the asymptotic decay rate since it is independent of the magnitude of the viscosity coefficients. No matter how small one makes the difference interval there is still a finite viscosity term in the equations.

This paradox can be resolved by considering a simple example. In one spatial dimension the planar response of a Voigt solid is governed by Eq. (25). The Green's function for a source at the origin is obtained by solving Eq. (25) with a source at the origin having a delta function time dependence. The solution for the Green's function is

$$G(x, t; 0, t') = \frac{A_0}{\sqrt{\nu x}} \exp \left[\frac{-\alpha^3}{2\nu x} (\tau - \tau')^2 \right] \quad (40)$$

where A_0 is a constant and τ is the retarded time. The spatial variable x has been used instead of r since planar rather than spherical geometry is being considered. The response for any kind of time dependence of the source $\psi_0(\tau')$ is then given by convolution with the Green's function

$$\psi(x, t) = \frac{A_0}{\sqrt{\nu x}} \int_{-\infty}^{\infty} \psi_0(\tau') \exp[-\beta(\tau - \tau')^2] d\tau', \quad (41)$$

where

$$\beta = \alpha^3/(2\nu x).$$

To make the example as simple as possible consider a rectangular time pulse of width $2a$. Then the solution is

$$\psi(x, t) = \frac{A_0}{\sqrt{\nu x}} \int_{\tau-a}^{\tau+a} \exp(-\beta\xi^2) d\xi = \frac{A_0}{\sqrt{\nu r\beta}} \int_{(\tau-a)\sqrt{\beta}}^{(\tau+a)\sqrt{\beta}} \exp(-y^2) dy. \quad (42)$$

Then, at the center of the pulse, the amplitude is

$$\psi_c = A_1 \int_{-a\sqrt{\beta}}^{a\sqrt{\beta}} \exp(-y^2) dy. \quad (43)$$

For large β corresponding to small x this reduces to

$$\psi_c(x) = A_2 \left[1 - \frac{1}{a} \sqrt{\frac{2\nu}{\pi\alpha^3}} \exp \left(-\frac{a^2\alpha^3}{2\nu x} \right) \left(\sqrt{x} - \frac{\nu x^{3/2}}{a^2\alpha^3} + \dots \right) \right], \quad (44)$$

and for small β corresponding to large x

$$\psi_c(x) = A_3 \left[a \sqrt{\frac{\alpha^3}{2\nu x}} - \frac{a^3}{3} \left(\frac{\alpha^3}{2\nu x} \right)^{3/2} + \dots \right]. \quad (45)$$

If the material response were purely elastic the rectangular pulse would simply maintain its shape and amplitude. In the visco-elastic case the pulse maintains its shape and amplitude during the initial stages of travel, except for a very slight rounding at the edges. Then there is a transition stage in which the pulse changes shape and its amplitude begins to decay. Finally, the asymptotic state is reached; the pulse shape assumes Gaussian form and the amplitude becomes inversely proportional to the square root of the range. How these different stages arise is easily understood by referring to the convolution integral Eq. (41). For short ranges the width of the Gaussian Green's function Eq. (40) is very narrow in comparison with the width of the rectangular pulse. Convolution with the rectangular pulse simply reproduces the rectangular pulse. When the range is sufficiently great the width of the Green's function becomes comparable to the width of the initial rectangular source pulse. Convolution then strongly alters the shape and amplitude of the initial pulse. Finally, at very great range the Gaussian Green's function becomes much wider than the initial rectangular pulse. Convolution of the two functions then simply reproduces the Green's function except for change of amplitude scale.

The viscosity ν appears in the solution Eq. (40) as a scale factor multiplying the range x . Thus, the effect of reducing the viscosity is to delay the onset of the asymptotic stage. By making the viscosity vanishingly small, the range at which the asymptotic stage begins can be made to approach infinity. This behavior explains why solutions obtained from numerical calculations with the traditional linear Q will converge to elastic solutions in the limit of vanishingly small difference interval. Unfortunately, practical computer calculations must be made with a finite mesh interval, usually large, perhaps no smaller than about 5% the width of the purely elastic disturbance. In decaying wave calculations, the transition to the asymptotic stage occurs well within the ranges of interest for practical choices of zoning.

Finally, it should be noted that the linear Q will affect the calculation of other types of decaying waves specific to solids. In particular, solids can support Rayleigh waves that propagate along a free surface rather than through the bulk of the solid. In the case of purely elastic behavior and a finite size source, these waves have an amplitude proportional to the inverse square root of the range; however, the traditional linear Q programs calculate amplitudes that are observed to be proportional to the inverse first power of the range. The results that have been obtained for surface waves will be published in a separate paper or made available in the form of a laboratory report.

ACKNOWLEDGMENTS

This work was supported by the U.S. Atomic Energy Commission and the Advanced Projects Research Agency. I would like to thank W. J. Hannon for allowing me to modify a copy of the

TENSOR program to the form suggested in this work. Also, I would like to thank John W. White and Barbara K. Crowley for their enthusiastic response to the original version of this paper which encouraged me to get on with the present revision.

REFERENCES

1. G. MAENCHEN AND S. SACK, The tensor code, *in* "Methods in Computational Physics," Vol. 3, pp. 181–210, Academic Press, New York, 1964.
2. J. T. CHERRY, S. SACK, G. MAENCHEN, AND V. KRANSKY, "Two-Dimensional Stress-Induced Adiabatic Flow," Lawrence Livermore Laboratory Report UCRL-50987 (1970).
3. M. L. WILKINS, Calculation of elastic-plastic flow, *in* "Methods in Computational Physics," Vol. 3, pp. 211–263, Academic Press, New York, 1964.
4. M. WILKINS, "Calculation of Elastic-Plastic Flow," Lawrence Livermore Laboratory Report UCRL-7322, Rev. I (1969).
5. R. D. RICHTMYER AND K. W. MORTON, "Difference Methods for Initial-Value Problems," 2nd ed., pp. 311–338, Interscience, New York, 1967.
6. M. J. LIGHTHILL, Viscosity effects in sound waves of finite amplitude, *in* "Surveys in Mechanics" (G. K. Batchelor and R. M. Davies, Eds.), pp. 250–351, Cambridge University Press, Cambridge, England, 1956.